

Measurement of Temperature-Induced Deformations in a Large Roof Structure

W. F. TESKEY, R. S. RADOVANOVIC, B. PAUL and R.G. BRAZEAL, Canada

Key words: temperature-induced deformations, large roof structure

SUMMARY

Deformation measurements on man-made structures are important because they provide a check on whether or not the structures are exhibiting safe deformation behaviour. These measurements are especially critical for large structures of unusual design. The roof of the Olympic Speed skating Oval in Calgary, Canada, which is one of the largest concrete space frame structures in the world, is such a structure. This structure experiences temperature-induced deformations because of the exposure to the outside of concrete buttresses which support the perimeter of the roof structure. A measurement scheme, consisting of two epochs of theodolite intersection observations to roof points, was used to measure these deformations. Theoretical temperature-induced deformations were also computed, and actual and theoretical deformations are shown to be in very close agreement. This close agreement between actual and theoretical temperature-induced deformations (which was also shown previously for deformations due to the dead weight load of the roof structure and deformations due to creep and shrinkage of the concrete in the roof beam columns) indicates that the structure is exhibiting a safe deformation behaviour. Preliminary results using a single-station reflectorless total station scheme are presented, and indicate serious distance errors may be present due to the varying reflector-ray geometries.

Measurement of Temperature-Induced Deformations in a Large Roof Structure

W. F. TESKEY, R. S. RADOVANOVIC, B. PAUL and R.G. BRAZEAL, Canada

1. INTRODUCTION

Deformation measurements on man-made structures are important because they provide a check on whether or not the structures are exhibiting safe deformation behaviour. These measurements are especially critical for large structures of unusual design.

The Olympic Speedskating Oval in Calgary is a very large, uniquely designed structure. It was built for the 1988 Winter Olympics. The Olympic Oval roof structure, with an unsupported span of approximately 80m by 200m, is one of the largest of its type in the world.

The roof structure of the Olympic Oval consists of 84 interconnected hollow-core beam columns. The external cross section of the beam columns is approximately 1m wide by 2m deep. The roof structure is hinged at the tops of buttressed columns, with both the columns and buttresses founded on concrete piles. The columns are approximately 1.5m in diameter and the buttresses are approximately 1.5m wide by 2m deep. Fig. 1(a) shows a cross section through the Olympic Oval and Fig. 1(b) shows the west elevation.

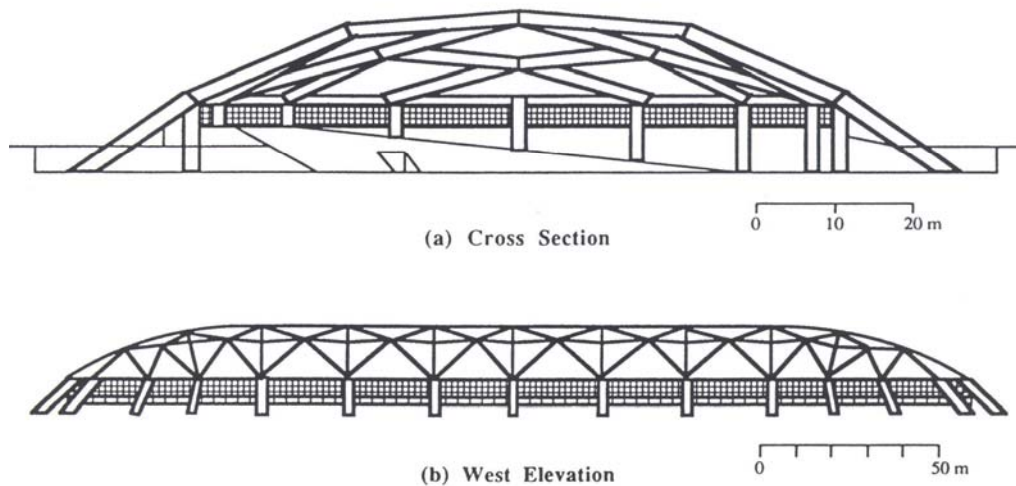


Figure 1: Olympic Oval, Calgary

The Olympic Oval has experienced both short-term and long-term deformations. The short-term deformations (deformations occurring as soon as the load is applied) are due to:

- Dead weight load of the structure itself.

- Snow load on the structure.
- Wind load on the structure.
- Temperature changes in the structure.

The long-term deformations are due to:

- Shrinkage of the concrete.
- Creep of the concrete and soil (progressively smaller deformations occurring over a period of time under constant loading conditions).
- Changes in soil stiffness because of variations in moisture content of the soil.

2. PREVIOUS MEASUREMENTS OF DEFORMATIONS

The first deformations of interest (those due to the dead weight load of the roof structure) occurred when the roof structure was lowered onto the buttressed column substructure in June 1986. These deformations, for the middle cross section, are shown in Fig. 2. Special survey instrumentation which was used to make the deformation measurements is described in Teskey (1988).

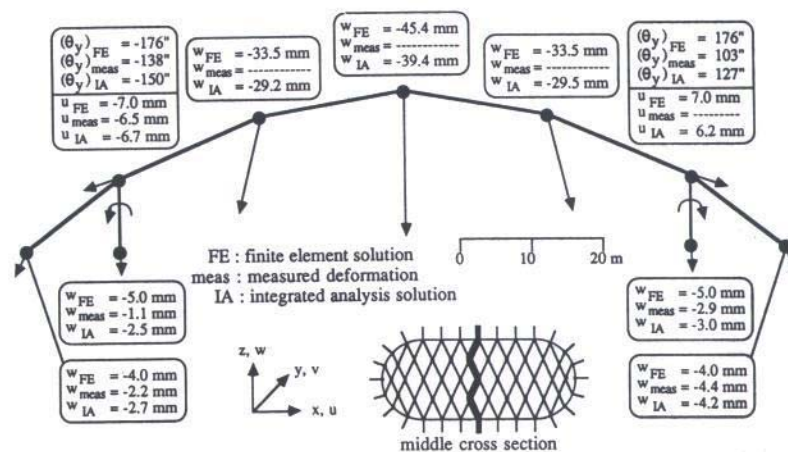


Figure 2: Deformations Due to Dead Weight Load of Roof, Middle Cross Section, Olympic Oval

Both translation and rotation deformations are shown in Fig. 2. Also shown in Fig. 2 are the actual measured deformations (denoted by “meas”), deformations computed by the structural finite element (denoted by “FE”) and deformations computed by integrated analysis (denoted by “IA”).

Integrated analysis is a computational method in which the structural finite element method is extended to incorporate actual measured deformations. As can be seen in Fig. 2, there is a significant change in the structural finite element solution produced by incorporating measured deformations into this solution by means of integrated analysis. The results show that the structural finite element solution produced displacements which were, in general, too

large. This means that for the loading due to the dead weight load of the roof, the structure is exhibiting a slightly safer deformation behaviour than that for which it was designed. Further details on the deformations due to the dead weight load of the roof structure are given in Teskey (1988).

Deformations of interest which occurred after the June 1986 dead weight load deformations were those due to creep and shrinkage of the concrete in the roof beam columns. These deformations, for the longitudinal centerline, are shown in Fig. 3. The deformations in Fig. 3 are labelled as “dH” to denote change in height.

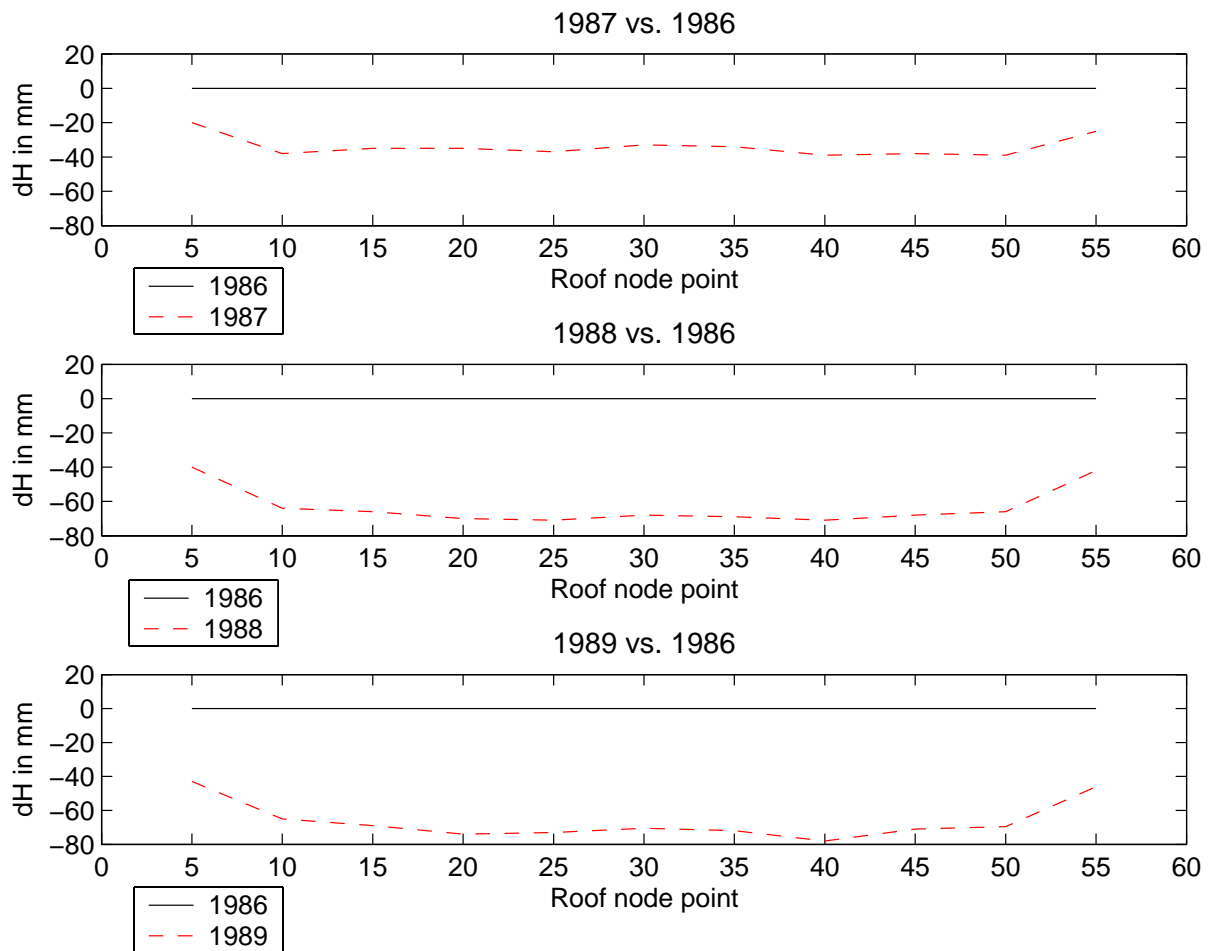


Figure 3: Longitudinal Centreline Displacements of Olympic Oval Roof Due to Creep and Shrinkage

The deformations were derived from four epochs of deformation survey measurements (August 1986, June 1987, June 1988, June 1989) which included, as target points, all the roof node points 2, 3, 4, 5, ... , 55, 56, 57, 58 inclusive shown in Fig. 4. Details of the survey measurements and methodology used to compute the deformations are given in Teskey (1991).

Fig. 3 shows clearly that the long-term deformation behaviour of the Olympic Oval roof due to creep and shrinkage of the concrete in the roof beam columns had almost completely stabilized by June 1989. The total downward displacement in the centre of the roof, from August 1986 (after the roof structure was lowered onto the buttressed column substructure) to June 1989 is about 7 cm. The magnitude of these deformations and the deformation pattern is in very good agreement with that predicted by the designers of the structure (Barry Lester, personal communication, June 4, 1985.)

3. MEASUREMENT OF TEMPERATURE-INDUCED DEFORMATIONS

3.1 Measurement Scheme

To measure temperature-induced deformations of the Olympic Oval roof, a simple and reliable measurement scheme was adopted. The measurement scheme consisted of two epochs of theodolite intersection observations to the roof points shown in Fig. 4. Theodolite intersection was adopted in this application because previous experience of the first author (Teskey and Wentzel 1989, Teskey 1992) and others indicated that standard deviations of three-dimensional coordinates could be determined to +/- 1mm or better with this method.

Targets at the roof points are extremely important in this measurement scheme. The targets used were those which were originally placed on the undersides of the roof nodes in 1986. The body of each target is a 40mm diameter plexiglass hemisphere. The hemisphere is flattened by three surfaces of equal width, each concentric about the axis of symmetry of the hemisphere. The flattening of the hemispherical body produces a well-defined target point at the tip of the target.

Reference points in the measurement scheme are shown in Fig. 4 and labelled as 201 and 202. Each reference point is a flat 30mm diameter concentric circle target epoxied to the concrete floor of the Olympic Oval. In each epoch, the following measurements were made: height of instrument (a Leica TC805 total station) at 201; spatial distance, horizontal and vertical circle readings from 201 to a tripod mounted reflector target set at 202; horizontal and vertical circle readings from 201 to the roof points; spatial distance, horizontal and vertical circle readings from 202 to 201 (after exchange of instrument and reflector target set between 201 and 202); horizontal and vertical circle readings from 202 to the roof points.

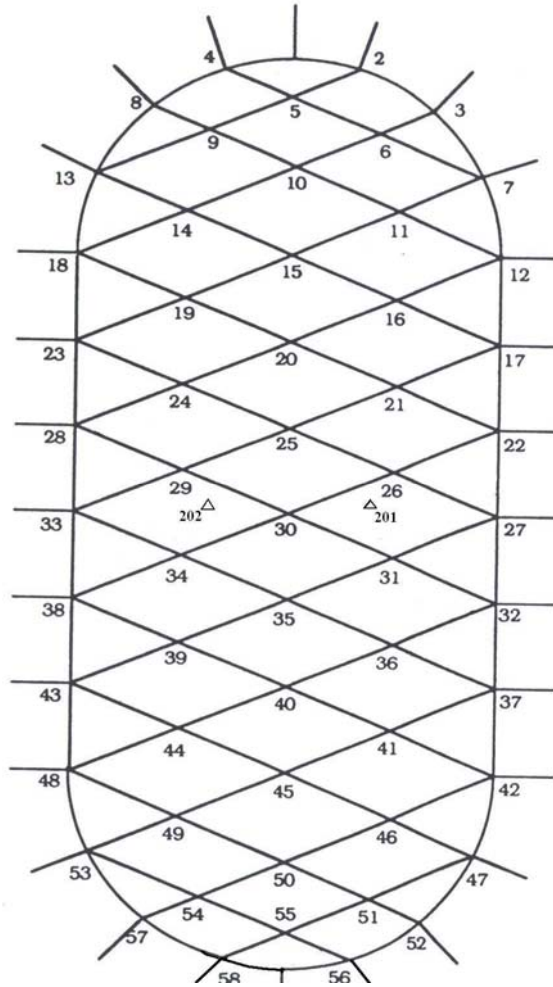


Figure 4: Plan View of Olympic Oval Roof

3.2 Results

The first measurement epoch was January 27/04 (outside air temperature -30 degrees Centigrade); the second measurement epoch was April 26/04 (outside air temperature $+20$ degrees Centigrade). Three-dimensional coordinates of the roof points, relative to floor points 201 and 202 were computed in each measurement epoch. These coordinates were then differenced to obtain movement of the roof points from January 27/04 to April 26/04. The largest movements of the roof points were upward displacements along the longitudinal centreline. These displacements, labelled as “dH” to denote change in height, are shown in Fig. 5.

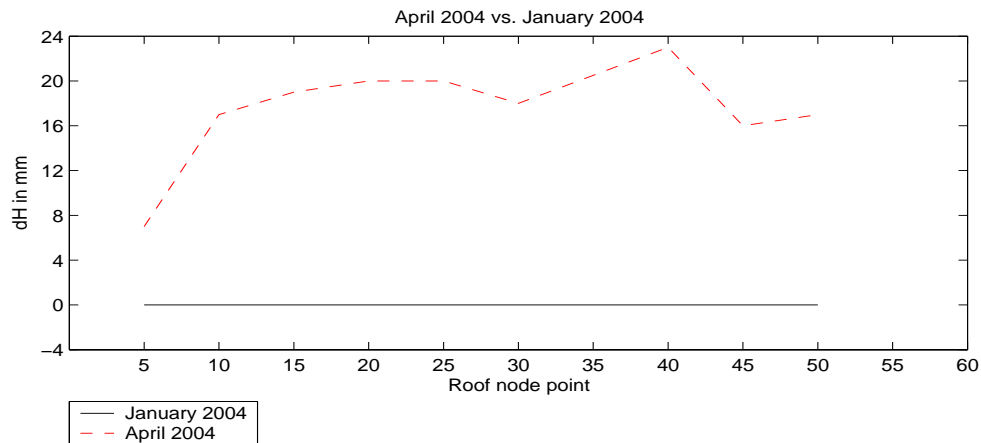


Figure 5: Longitudinal Centreline Displacements of Olympic Oval Roof Due to Seasonal Temperature Change

4. COMPUTATION OF THEORETICAL TEMPERATURE-INDUCED DEFORMATIONS

Theoretical temperature-induced deformations along the longitudinal centerline of the Olympic Oval roof can be computed by considering the geometry of the roof and supporting buttresses, along with the -30 degrees Centigrade to $+20$ degrees Centigrade temperature change and the coefficient of linear thermal expansion for the concrete buttresses.

An approximation of the Olympic Oval roof geometry for a typical cross-section is shown in Fig. 6. In this figure, the total distance along the roofline is l (the distance from the tops of the buttresses at the perimeter of the roof to the highest point on the roof is $l/2$); the horizontal distance from the top of a buttress on one side of the roof to the top of the buttress on the other side of the roof is b (the horizontal distance from the top of a buttress to the location vertically below the highest point on the roof is $b/2$); the height of the highest point on the roof, relative to the horizontal line connecting buttresses on opposite sides of the roof, is h .

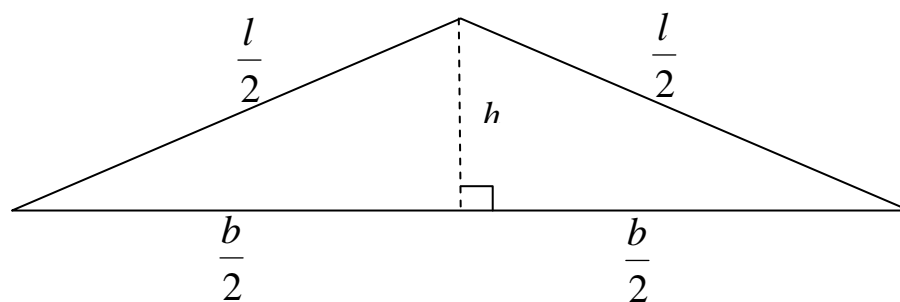


Figure 6: Roof Geometry

From Fig. 6, the equation of h as a function of l and b is:

$$h = \left(\left(\frac{l}{2} \right)^2 - \left(\frac{b}{2} \right)^2 \right)^{\frac{1}{2}} \quad (1)$$

Taking the first derivative of h with respect to l :

$$\frac{dh}{dl} = \frac{l}{4h} \quad (2)$$

Rearranging Eqn. (2) in order to express dh , a change in height at the highest roof point, as a function of dl , a change in length along the roofline:

$$dh = \frac{l}{4h} dl \quad (3)$$

The relationship between dh and dl can also be developed geometrically by considering the original position of the highest roof point, and the new position of the highest roof point after there is a change in length along the roofline. Refer to Fig. 7. In Fig. 7, the slope of the roof on each side of the highest point is $l/2$ units on the slope to h units vertical. As can be seen in Fig. 7, the $l/2 - h$ right angle triangle also gives the relationship between dh , change in height at the highest roof point, and dl , change in length along the roofline. With reference to Fig. 7, by similar triangles,

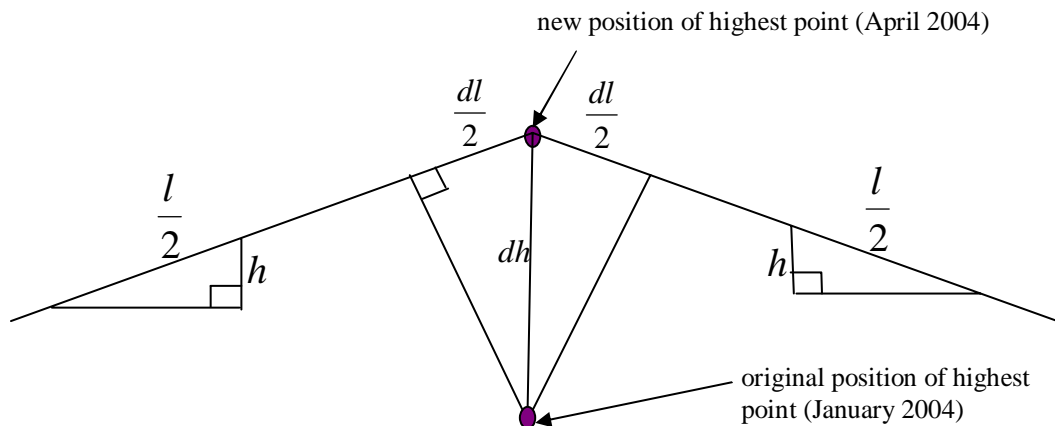


Figure 7: Original and New Positions of Highest Point

$$dh / (dl/2) = (l/2) / h \quad (4)$$

After rearranging equation (4),

$$dh = \frac{l}{4h} dl \quad (5)$$

which is identical to the relationship developed mathematically from Fig. 6.

The upward movement of the Olympic Oval roof from January 2004 to April 2004 was caused by a temperature-induced change in length of the buttresses which support the roof structure. These buttresses are exposed and thus subject to the outside air temperature. The entire roof structure is indoors. It is completely insulated from above and subject to a year-round air temperature of about 20 degrees Centigrade. This means that the change in length of the roof structure, shown in Fig. 7 as $(dl/2 + dl/2)$ symmetrical about the highest point, actually occurs at the tops of the buttresses at the perimeter of the roof structure.

With the relationship between dh and dl established by identical equations (3) and (5), the next step is to compute dl . This can be done with the following equations:

$$dL = L \times a \times (dT) \quad (6)$$

in which dL is the change in length of the two buttresses at the perimeter of a roof cross-section;

L is the length of the two buttresses;

a is the coefficient of linear thermal expansion for the concrete buttresses;

dT is the change in temperature;

and $dl = dL \cos(\text{gamma})$ (7)

in which dl is the change in length along the roofline;

dL is defined above;

(gamma) is an angle representing the difference in slope between the buttresses and the roof cross-section.

The angle (gamma) is required to compute the component of dL which is aligned with the roofline. As can be seen in Fig. 1, the slope of the buttresses is not the same as the slope of the roofline.

Using the values $dT = +50$ degrees Centigrade, $a = 0.000\ 010$ per degree Centigrade (Troxell et al. 1968), $L = 24.0\text{m}$, $(\text{gamma}) = 20$ degrees, $l = 80\text{m}$ and $h = 10\text{m}$ in Eqns (5), (6) and (7), the change in height dh of the highest roof point is 23mm.

5. COMPARISON OF ACTUAL AND THEORETICAL DEFORMATIONS

Actual measured temperature-induced displacements on the longitudinal centerline of the Olympic Oval roof are shown in Fig. 5. The average value of the displacements of the roof node points on full cross-sections is 19mm. (See Fig. 4: roof node points on full cross-sections are 15, 20, 25, 30, 35, 40 and 45; roof node points not on full cross-sections are 5, 10, 50 and 55.) This average value of 19mm can be compared to the theoretical value of 23mm computed in the previous section.

The discrepancy between actual and theoretical values could be due to small errors in the parameters in Eqns (5), (6) and (7) which are used to compute the theoretical value of 23mm. The values assigned to these parameters are likely correct to within 5% or better of their true values, except for the coefficient of linear thermal expansion which might be in error by as much as 10%. Actual measured displacements are expected to be correct (no systematic errors), with a standard deviation of about ± 1 mm for roof node points 25, 30 and 35 and a standard deviation of about ± 2 mm for roof node points 15, 20, 40 and 45. The expectation of no systematic errors and small standard deviations for measured displacements is based on previous experience of the first author with the theodolite intersection method (Teskey and Wentzel 1989, Teskey 1992) plus the fact that that with theodolite intersection two independent observations of heights of roof points are possible in each measurement epoch. In this application, the two independently observed heights were typically different by less than 1.0mm, and the average value was adopted.

The discrepancy between actual and theoretical values could also be due to the fact that the entire 1.5m wide by 2m deep cross-section of the concrete buttresses probably had not reached the ambient temperature of +20 degrees Centigrade when the April 2004 measurements were made. Were this the case, actual displacements would be less than measured displacements.

6. COMPARISON WITH REFLECTORLESS TOTAL STATION

As the Olympic Oval is a year-round operating facility, is it crucial that deformation monitoring surveys disrupt operations as little as possible. Theodolite intersection is a time-intensive process, and as a result the authors investigated the possibilities of using a reflectorless total-station at a single station to determine the roof node heights. It should be noted here that the reflective covering of the roof node targets does not produce sufficient return for a standard EDM measurement to be made.

In this test, a Leica TCR 702 reflectorless theodolite was set up over point 201, and the elevation of the station precisely determined using a level equipped with a parallel-plate micrometer. Distance and angular measurements were then made to a subset of roof node points and the elevations of these points determined. The test was conducted on June 25, 2004 (ambient outside temperature 20°C), so it was expected that the resulting roof node elevations should be identical to those determined during the April 26 test. Discrepancies between the two sets of elevations were computed and are shown graphically in Figure 8.

As can be seen, discrepancies in elevations up to 12 mm are evident, and in the majority of cases, the elevation derived from the reflectorless total-station is lower than that derived from theodolite intersection. Interestingly, further investigation of the zenith angles collected during the June 25 data set indicated that, based on a comparison of the observed zenith angles with the “theoretical” angles computed using coordinates derived from theodolite intersection, the expected discrepancies in roof node elevations should not exceed 2 mm. The listed standard deviation of the Leica 702 instrument operating in reflectorless mode is 3 mm. Thus the observed discrepancies are far beyond what would be expected due to normal observational error.

Figure 9 shows the relationship between observed zenith angle to the roof nodes and the “apparent distance error.” This error is computed by determining the theoretical slope distance between the instrument and roof node points assuming using coordinates derived from theodolite intersection and subtracting this quantity from the actual distance observed. For roof node points located near the horizon, the scatter in the apparent distance errors becomes larger, and reaches 28 mm. As well, one roof point node shows a large positive distance error.

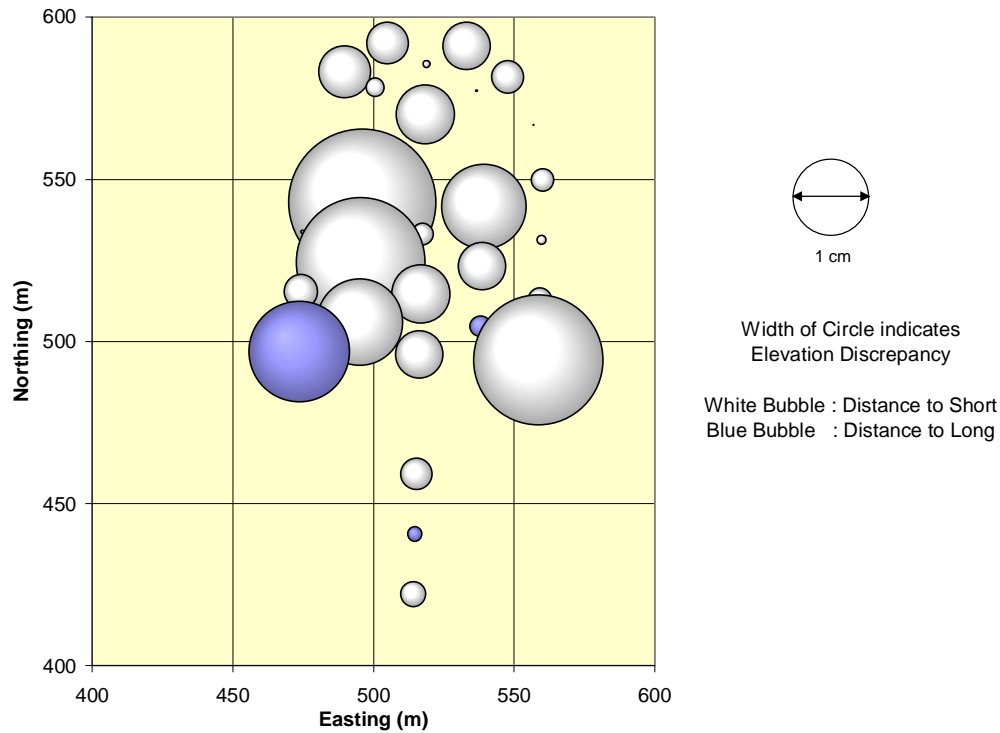


Figure 8: Discrepancies between Elevations Measured via Reflectorless Total-station and Theodolite Intersection

One possible explanation for this behaviour lies in the geometry of the reflector and ray. Figure 10 shows two typical situations. In the first case, the EDM beam strikes the reflector directly at the point sighted, resulting in a “correct” distance. In the latter case, the EDM beam strikes the reflector laterally, so that the distance returned is too short. The beam of the EDM on the Leica 702 has an up/down width of 55 mm at 107 m standoff distance (Rueger, 2003) and if one assumes that the distance reported by the EDM is the “time of first return”, the distance could be shorter by up to 2 cm due to illumination of the leading edge of the target. Unfortunately, since the targets are mounted flush to the bevelled roof supports, the orientation of the reflector with respect to the theodolite cannot be expressed by a simple zenith angle function. Further work is required to verify if this effect can explain the large EDM errors apparent.

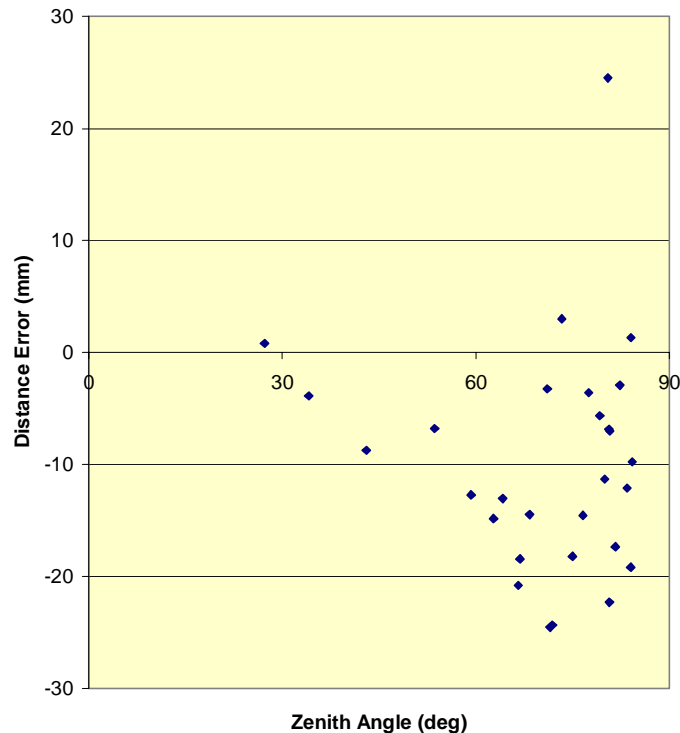


Figure 9: Comparison of Apparent Distance Error and Zenith Angle

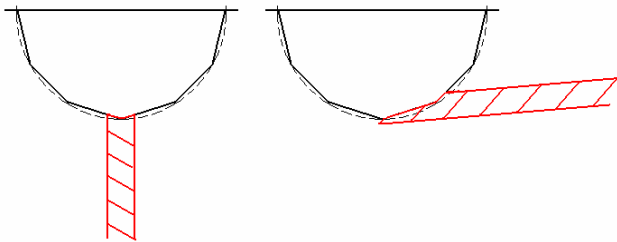


Figure 10: Reflector / Ray Geometries

Fortunately, since deformations are expected to be relatively small (i.e. on the order of 2 centimetres), the reflector/ray geometry will not significantly change and thus the EDM error will remain constant between epochs. This implies that, while establishment of accurate relative heights of roof points using the reflectorless EDM is not possible, relative movements between epochs of individual points may be measured. This hypothesis was indeed verified by adjusting the height of the station by known amounts and re-observing the roof node points with the reflectorless total-station. Station height changes (up to 4 cm) were recovered to the 1 mm level.

7. FUTURE WORK

In the near future it is planned to investigate other measurement schemes to determine structural deformations. The first measurement scheme will consist of two epochs of

reflectorless total station observations to the Olympic Oval roof points; the second measurement scheme will consist of multiple epochs of laser scanner observations to the entire Olympic Oval roof, including the roof points. Special features of reflectorless total stations and laser scanners, which are important for deformation monitoring applications, are described in Rueger (2003).

Both of these measurement schemes offer an advantage over theodolite intersection in terms of time required for data acquisition. This is a critical advantage in cases where catastrophic failure might be possible, e.g. the recent Terminal 2E roof collapse at Charles de Gaulle Airport near Paris (Broughton 2004).

8. CONCLUSION

Measurement of temperature-induced deformations in the Olympic Oval roof produced a result which was very close to the theoretical result. Previous measurements of deformations (those due to the dead weight load of the roof structure and those due to creep and shrinkage of the concrete in the roof beam columns) also produced results which were very close to the theoretical results. All of these measurements of deformations indicate that the structure is exhibiting a safe deformation behaviour.

ACKNOWLEDGEMENTS

The authors would like to thank Kameron Kiland for arranging access to the Olympic Oval facility. Research funding provided by the Natural Sciences and Engineering Research Council of Canada is gratefully acknowledged. Funding by the Alberta Land Surveyors' Association allowed the presentation of this paper and is appreciated.

REFERENCES

- Broughton, P. D. (2004). "Roof Collapse Kills Five at Paris Air Terminal", Calgary Herald (from The Telegraph, Paris), May 24, p. A8.
- Rueger, J. M. (2003). "Electronic Surveying Instruments", Monograph 18, School of Surveying and Spatial Information Systems, The University of New South Wales, Sydney, 155 pp.
- Teskey, W. F. (1988). "Special Survey Instrumentation for Deformation Measurements", Journal of Surveying Engineering, Vol. 114, No. 1, pp. 2-12.
- Teskey, W. F. (1991). "Geometrical Deformation Analysis of a Large Roof Structure", Journal of Surveying Engineering, Vol. 117, No. 1, pp. 36-49.
- Teskey, W. F. (1992). "Trigonometric Levelling in Precise Engineering Surveys", Surveying and Land Information Systems, Vol. 52, No. 1, pp. 46-53.
- Teskey, W. F. and Wentzel, J. F. (1989). "A method of Precise Trigonometric Levelling for Deformation Surveys", CISM Journal ACSGC (now Geomatica), Vol. 43, No. 4, pp. 357-365.
- Troxell, G. E., Davis, H. E. and Kelly, J. W. (1968). "Composition and Properties of Concrete", McGraw-Hill, New York, 529 pp.

BIOGRAPHICAL NOTES

Bill Teskey is a Professor in the Department of Geomatics Engineering at the University of Calgary. He is a registered professional in Alberta, and a registered land surveyor in Alberta and Canada. His research area of interest is high-precision industrial surveys.

Robert Radovanovic is the owner of SARPI LTD, a surveying company based in Alberta, Canada. He received his Ph.D. at the University of Calgary and is a registered land surveyor in Alberta and Canada. His research area is deformation monitoring and the application of global navigation systems to high-precision surveying.

Bijoy Paul is an MSc Graduate Student in the Department of Geomatics Engineering at the University of Calgary. His research area of interest is high-precision industrial surveys.

Ryan Brazeal is a Geomatics Engineer with Focus Corporation Ltd. In Regina, Saskatchewan. He plans to return to the Department of Geomatics Engineering at the University of Calgary in 2005 to start an MSc program in high-precision industrial surveys.

CONTACTS

W. F. Teskey, R. S. Radovanovic, B. Paul and R.G. Brazeal
Dept. of Geomatics Engineering, University of Calgary
2500 University Drive N. W.
Calgary, AB
CANADA
Tel. + 1 403 220 5834
Fax + 1 403 284 1980
Email: wteskey@ucalgary.ca, rsradova@ucalgary.ca,
bpaul@ucalgary.ca, rgbrazea@ucalgary.ca